Turkish J. Eng. Env. Sci.
32 (2008) , 211 – 218.

Direct and Indirect Extrusion of Sintered Preform at the End of Stroke

Abhay Kumar SHARMA
Mechanical Engineering Department, BRCM CET, Bahal Bhiwani, 127028 INDIA
e-mail-rkranjanbit@yahoomail.com
Rajesh Kumar RANJAN
Mechanical Engineering Department, BRCM CET, Bahal Bhiwani, 127028 INDIA
V. K. BAJPAI
Mechanical Engineering Department, NIT, Krukshetra-INDIA

Received 05.02.2008

Abstract

The paper reports a theoretical investigation into various aspects of cold forming through conical converging die at the end of stroke. At this stage of the process, there occur some phenomena that require discussion. A well-known defect in extrusion is cavity formation at the center on the back of the billet, a process that begins as the billet is shortened. The cavity gradually increases in diameter and depth, transforming the emerging rod into a pipe of increasing inner diameter, with the result that this portion of the product is discarded. This defect can be reduced or eliminated if dies of smaller cone angles are used. The results so obtained are discussed critically to illustrate the interaction of various process parameters involved and are presented graphically.

Key words: Sintered preform, Upper bound approach, Inter-facial friction, Strain Rates, Velocity Fields

Introduction

During the last few years, metal-powder components have assumed an important position in industry, as they are used successfully in a wide range of applications. Both the mechanical and the metallurgical properties of the metal powder components compare favorably with those of wrought materials (Ramakrishna, 1980; Jha et al., 1994; Singh et al., 2001; Ilia et al., 2005). Bulk processing of metal powder preforms is a convenient method of reducing or eliminating the porosity from conventional powder metallurgy products. The process is attractive because it avoids large numbers of operations, high scrap losses, and high-energy consumption associated with the conventional manufacturing processes such as casting and machining. In this new technology sintered porous powder preforms are used as starting materials in metal forming processes. Metal powder products manufactured by this new technology are comparable and in some cases even superior to cast and wrought products.

Although a considerable amount of work has been reported recently on the various technological aspects of the industrial processing of metal-powder preforms (Tabata et al., 1980; Jha et al., 1984; Agrawal et al., 1999; Kumar et al., 2001), no systematic attempt has been made so far to study the processing load and deformation characteristics at the end of stroke.

As shown in Figure 1, the pressure goes through a minimum and then a rapid increase near the end of stroke. At this stage of the process, there occur some phenomena that require discussion. A well-known defect in extrusion is cavity formation at the center on the back of the billet, a process that begins as the billet is shortened. The cavity gradually increases in diameter and depth, transforming the emerging rod

into a pipe of increasing inner diameter, with the result that this portion of the product is discarded. This defect can be reduced or eliminated if dies of smaller cone angles are used.

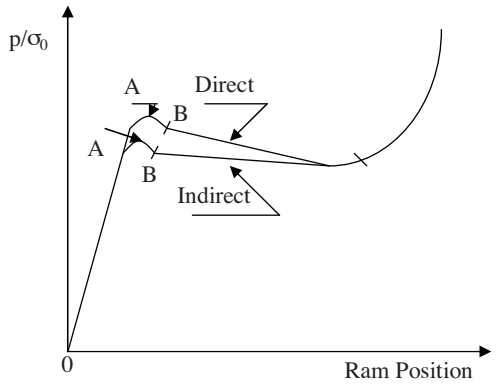

Figure 1. Characteristic ram pressure curve.

As the piston penetrates deeper into zone-II, at a radial distance r smaller than r_0 (Figure 2), the billet velocity at the center of symmetry exceeds v_0, the velocity of the piston on contact. The material at the center thus breaks contacts with the piston, and a cavity begins to form. At more advanced stages, the spherical velocity field is no longer kinematically admissible and has to be replaced. The kinematically admissible velocity field for direct and indirect extrusion with square dies is shown in Figure 2.

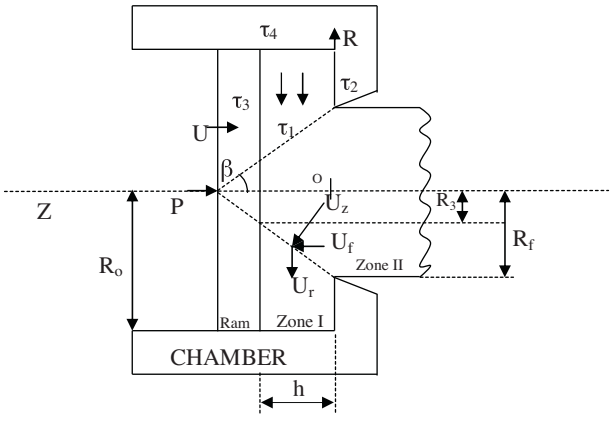

Figure 2. Kinematically admissible velocity field for the end of stroke.

The velocity field loses its meaning near the end of the extrusion stroke. Zone-II represents a pipe moving axially as a rigid body at an arbitrary velocity v_f, while zone-I is a body in plastic flow. The velocity field in zone-I can be described as a parallel field.

It is expected that the present work will be of great importance for the assessment of relative extrusion stress developed at the end of stroke during the flow through conical converging dies of metal powder preforms.

Yield Criteria and Plastic Deformation

In an investigation of the plastic deformation of metal-powder preforms, it is evident that with the application of compressive hydrostatic stress the pores will close and the relative density will increase, whereas with the application of tensile hydrostatic stress the pores will grow and the relative density will decrease. The density distribution also does not seem to be uniform throughout, being high in the central region and low at the edges. The density distribution will be more uniform for a smaller coefficient of friction μ and for a greater initial density (Deryagin et al., 1952).

Tabata et al. (1980) proposed the following yield criterion for porous metal powder preforms:

$$\rho^k = \sqrt{3J_2'} \pm 3\eta\sigma_m \qquad (1)$$

The negative sign is taken for $\sigma_m \leq 0$ and the positive sign is taken for$\sigma_m > 0$.

Figure 3 shows that the yield surface for a porous metal powder preform given by the above equation consists of 2 cones, the height of the cones increasing with increasing ρ. When $\rho = 1$, i.e. a pore-free metal, the cone becomes a cylinder and the equation reduces to the von Mises yield criterion. The values of η and k were determined experimentally from simple compression and tension tests of sintered copper-powder preforms (Deryagin et al., 1952) as

$$\eta = 0.54\,(1-\rho)^{1.2} \text{ for } \sigma_m \leq 0$$

$$\eta = 0.55\,(1-\rho)^{0.83} \text{ for } \sigma_m > 0 \text{ and } k = 2$$

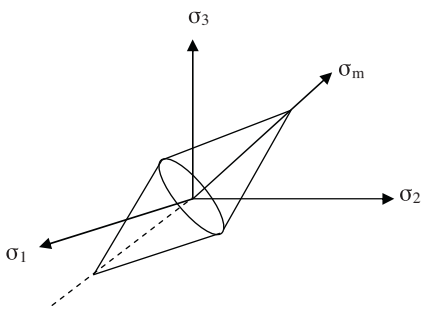

Figure 3. Yield surface for porous metal powder perform.

For the axisymmetric condition the yield criterion reduces to

$$\sigma_1 = \frac{\rho^k \sigma_0}{(1-2\eta)} + \frac{(1+\eta)}{(1-2\eta)}\sigma_2 \text{ (for negative sign)} \quad (2)$$

During the forming of metal-powder preforms the compressive force gradually increases the relative density, which later is directly proportional to the real area of contact. The relative density gradually approaches the apparent relative density (Figure 4), with this approach probably being asymptotic (Rooks, 1974).

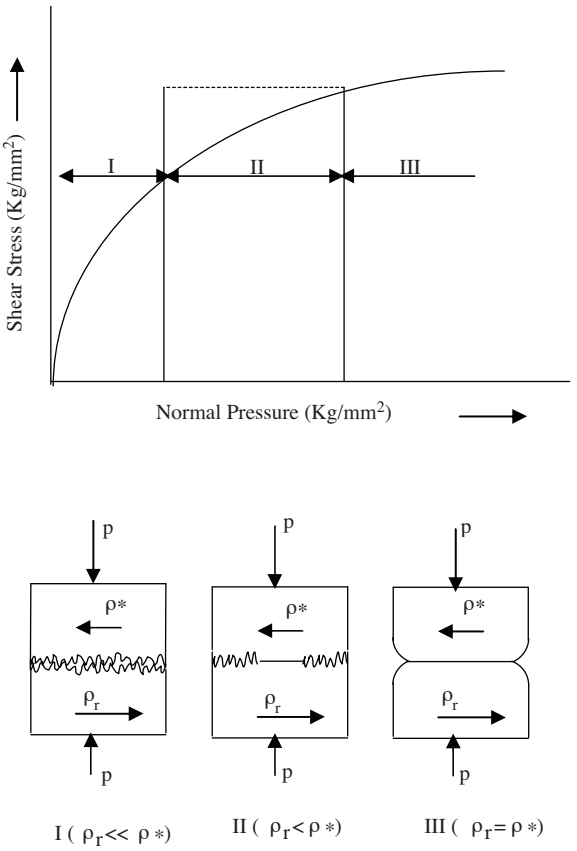

Figure 4. Three regimes of density variation.

Friction conditions between the deforming tool and work piece in metal forming are of the greatest importance in terms of a number of factors such as force and mode of deformation, properties of the finished specimen, and resulting surface roughness. During the sinter forging process it is very important to pay special attention to the interfacial friction, as this will determine the success or failure of the operation.

Velocity Field

Its velocity field is similar to that of a hollow disk having

$$R_n = R_0$$

$$U_\theta = 0$$

$$U_z = \frac{Uz}{h}$$

$$U_r = -\frac{(1-2\eta)\,Ur}{2\,(1+\eta)\,h}\left[1-\left(\frac{R_0}{R}\right)^2\right] \quad (3)$$

Strain Rates

$$\dot{\varepsilon_r} = -\frac{(1-2\eta)\,U}{2\,(1+\eta)\,h}\left[1+\left(\frac{R_0}{R}\right)^2\right]$$

$$\dot{\varepsilon_r} = -\frac{(1-2\eta)\,U}{2\,(1+\eta)\,h}\left[1-\left(\frac{R_0}{R}\right)^2\right]$$

$$\dot{\varepsilon_z} = \frac{U}{h}$$

$$\dot{\varepsilon_{r\theta}} = \dot{\varepsilon_{\theta z}} = \dot{\varepsilon_{zr}} = 0 \quad (4)$$

Velocity Discontinuity

Along Γ_1

$$\Delta v = U_r \sin\beta + (v_f - U_z)\cos\beta$$

$$= -\frac{(1-2\eta)\,Ur}{2\,(1+\eta)\,h}\left[1-\left(\frac{R_0}{R}\right)^2\right]\sin\beta + \left(v_f - \frac{z}{h}U\right)\cos\beta$$

Along Γ_2 and Γ_3

$$\Delta v = U_r = -\frac{(1-2\eta)\,Ur}{2\,(1+\eta)\,h}\left[1-\left(\frac{R_0}{R}\right)^2\right]$$

Along Γ_4

$$\Delta v = U_z = \frac{Uz}{h} \quad (5)$$

Surface of Velocity Field

The normal components of both velocity fields (in zone-I and in zone-II) must be equal along the surface Γ_1. This requirement dictates the geometry of Γ_1 and it is written as

$$v_f \sin\beta = U_R \cos\beta + U_z \sin\beta$$

$$\text{or } \cot\beta = \frac{v_f - U_z}{U_R} = -\frac{dz}{dR} \tag{6}$$

Inserting the values of U_z and U_R in Eq. (6)

$$-\frac{dz}{dR} = \frac{v_f - \frac{z}{h}U}{-\frac{(1-2\eta)Ur}{2(1+\eta)h}\left[1-\left(\frac{R_0}{R}\right)^2\right]} \tag{7}$$

Equation (6) is solved by separation of the variables as follows:

$$\frac{2(1+\eta)h}{(1-2\eta)}\frac{rdr}{R_0^2 - R^2} = -\frac{dz}{v_f - \frac{U}{h}z}$$

The solution of this equation is

$$\begin{aligned} &-\frac{(1+\eta)h}{(1-2\eta)U}\left(R_0^2 - R^2\right) - \frac{(1+\eta)h}{(1-2\eta)U}\ln C \\ &= \frac{h}{U}\ln\left(v_f - \frac{h}{U}z\right) \\ &\Rightarrow \frac{(1+\eta)h}{(1-2\eta)U}\left(R_0^2 - R^2\right)C\left(\frac{U}{h}z - v_f\right) = 1 \end{aligned} \tag{8}$$

From the boundary condition, $R\,|_{z=0} = R_f$

$$C = -\frac{(1-2\eta)}{(1+\eta)\left(R_0^2 - R_f^2\right)v_f} \tag{9}$$

Substituting the value of C in the above equation,

$$R = R_f\sqrt{\frac{1-\left(\frac{R_0}{R_f}\right)^2\left(\frac{U}{v_f}\right)\left(\frac{z}{h}\right)}{1-\left(\frac{U}{v_f}\right)\left(\frac{z}{h}\right)}}$$

where

$$\tan\beta = \frac{U_r}{v_f - U_z} = -\frac{\frac{(1-2\eta)Ur}{2(1+\eta)h}\left[1-\left(\frac{R_0}{R}\right)^2\right]}{v_f - \frac{Uz}{h}}$$

$$\Rightarrow \tan\beta = -\frac{(1-2\eta)Ur}{2(1+\eta)}\frac{\left[1-\left(\frac{R_0}{R}\right)^2\right]}{(hv_f - Uz)} \tag{10}$$

and the inner radius becomes

$$\frac{R_i}{R_0} = \sqrt{\frac{\left(\frac{R_f}{R_0}\right)^2 - \frac{U}{v_f}}{1-\frac{U}{v_f}}} \tag{11}$$

To make the boundary Γ_1 admissible, its geometry must follow Eq. (10), where the velocity v_f is still arbitrary.

Internal Power of Deformation

The internal power of deformation can be approximated by assuming zone-1 to be a hollow disk with a constant radius of

$$R_a = \frac{R_i + R_f}{2} \tag{12}$$

In this case,

$$dW_i = \frac{2}{\sqrt{3}}\sigma_0 \int_{R=R_a}^{R_0} \sqrt{\frac{1}{2}\dot{\varepsilon}_{ij}\dot{\varepsilon}_{ij}}dv$$

$$W_i = -\sqrt{\frac{3(1+\eta^2)}{2(1+\eta)^2}}R_0^2\frac{2\sqrt{2}}{\sqrt{3}}\pi\sigma_0 U$$

$$\left[\sqrt{1+\frac{(1-2\eta)^2}{3(1+\eta^2)}} - \sqrt{\left(\frac{R_a}{R_0}\right)^4 + \frac{(1-2\eta)^2}{3(1+\eta^2)}} - \sqrt{\frac{(1-2\eta)^2}{3(1+\eta^2)}}\times \ln\left\{\frac{\left(\frac{R_a}{R_0}\right)^2\left(\sqrt{1+\frac{(1-2\eta)^2}{3(1+\eta^2)}}+\sqrt{\frac{(1-2\eta)^2}{3(1+\eta^2)}}\right)}{\sqrt{\left(\frac{R_a}{R_0}\right)^4+\frac{(1-2\eta)^2}{3(1+\eta^2)}}+\sqrt{\frac{(1-2\eta)^2}{3(1+\eta^2)}}}\right\}\right] \tag{13}$$

Frictional Power of Deformation

Along Γ_1:

The power consumed along Γ_1 is computed as follows:

Δv along Γ_1:

$$= -\frac{(1-2\eta)Ur}{2(1+\eta)h}\left[1-\left(\frac{R_0}{R}\right)^2\right]\sin\beta + \left(v_f - \frac{zU}{h}\right)\cos\beta$$

Element of Shear Stress:

$$ds = 2\pi R\frac{dR}{\sin\beta}$$

$$\text{Theshear stress is } \tau = \frac{\sigma_0}{\sqrt{3}}$$

$$W_{s1} = \int_{\tau} | v | ds$$

$$= \int_{R=R_i}^{R_f} \left[-\frac{(1-2\eta)\, Ur}{2(1+\eta)\, h} \frac{\sigma_0}{\sqrt{3}} \left[1 - \left(\frac{R_0}{R} \right)^2 \right] \sin\beta + \left(v_f - \frac{zU}{h} \right) \cos\beta \right] 2\pi R \frac{dR}{\sin\beta}$$

The solution of the second integral is very involved. For simplification it will only be approximated. Since$v_f >> \left(\frac{U}{L}\right) z$, the term $\left(\frac{U}{L}\right) z$is neglected. Furthermore, let cotβ be considered constant and of the value of cotβ at R = R$_a$ so that

$$\cot\beta = -2 \frac{\left(\frac{L}{R_a}\right)\left(\frac{v_f}{U}\right)}{\left[1 - \left(\frac{R_0}{R_a}\right)^2\right]}$$

Now W$_{s1}$ is approximated as

$$W_{s1} = \frac{\pi\sigma_0(1-2\eta)UR_0^2}{\sqrt{3}(1+\eta)} \left[\frac{1}{3}\frac{R_0}{h} \left\{ \left(\frac{R_f}{R_0}\right)^3 - \left(\frac{R_i}{R_0}\right)^3 \right\} - \left(\frac{R_f}{R_0} - \frac{R_i}{R_0} \right) \right] - \frac{\pi\sigma_0 UR_0^2}{\sqrt{3}} \left[\left(\frac{v_f}{U}\right)^2 \left\{ \left(\frac{R_f}{R_0}\right)^2 - \left(\frac{R_i}{R_0}\right)^2 \right\} \right] \left[\frac{(h/R_a)}{1-(R_0/R_a)^2} \right] \quad (14)$$

Along Γ_2:

$$W_{s2} = -\frac{(1-2\eta)\, Um\sigma_0\pi}{3\sqrt{3}(1+\eta)\, h} \left[\frac{R_f}{R_0} \left\{ 3 - \left(\frac{R_f}{R_0}\right)^2 \right\} - 2 \right]$$

Putting R$_f$ = R$_a$

$$W_{s2} = -\frac{(1-2\eta)\, Um\sigma_0\pi R_0^3}{3\sqrt{3}(1+\eta)\, h} \left[\frac{R_a}{R_0} \left\{ 3 - \left(\frac{R_a}{R_0}\right)^2 \right\} - 2 \right] \quad (15)$$

Along Γ_3:

$$W_{s3} = -\frac{(1-2\eta)\, Um\sigma_0\pi R_0^3}{3\sqrt{3}(1+\eta)\, h} \left[\frac{R_i}{R_0} \left\{ 3 - \left(\frac{R_i}{R_0}\right)^2 \right\} - 2 \right]$$

Putting R$_i$ = R$_a$

$$W_{s3} = -\frac{(1-2\eta)\, Um\sigma_0\pi R_0^3}{3\sqrt{3}(1+\eta)\, h} \left[\frac{R_a}{R_0} \left\{ 3 - \left(\frac{R_a}{R_0}\right)^2 \right\} - 2 \right] \quad (16)$$

Along Γ_4

$$W_{s4} = -\pi R_0 m\sigma_0 Uh \quad (17)$$

According to mass constancy,

$$U = \rho \left(\frac{R_f}{R_0}\right)^2 v_f; \text{ and } \frac{U}{v_f} = \rho \left(\frac{R_f}{R_0}\right)^2 \quad (18)$$

Die Load

For plastic deformation of a metal powder the external power $\overset{*}{J}$ supplied by the ram is given as

$$\overset{*}{J} = W_i + W_{s1} + W_{s2} + W_{s3} + W_{s4}$$

and also $\overset{*}{J} = -\pi R_0^2 p_{ram} U$

$$\frac{p_{ram}}{\sigma_0} = -\sqrt{\frac{3(1+\eta^2)}{2(1+\eta)^2}} R_0^2 \frac{2\sqrt{2}}{\sqrt{3}} \left[\sqrt{1+A} - \sqrt{\left(\frac{R_a}{R_0}\right)^4 + A} - \sqrt{A} \ln \left| \frac{\left(\frac{R_a}{R_0}\right)^2 \left\{ \sqrt{1+A} - \sqrt{A} \right\}}{\sqrt{\left(\frac{R_a}{R_0}\right)^4 + A} + \sqrt{A}} \right| \right] + \frac{1}{\sqrt{3}} \left[\begin{array}{l} \left\langle \frac{(1-2\eta)}{3(1+\eta)} \left(\frac{R_0}{h}\right) \left\{ \left(\frac{R_f}{R_0}\right)^3 - \left(\frac{R_i}{R_0}\right)^3 \right\} - \left(\frac{R_f}{R_0} - \frac{R_i}{R_0} \right) \right\rangle + \left(\frac{v_f}{U}\right)^2 \left\{ \left(\frac{R_f}{R_0}\right)^2 - \left(\frac{R_i}{R_0}\right)^2 \right\} \\ \times \left\{ \frac{(h/R_a)(R_0/R_a)}{1-(R_0/R_a)^2} \right\} \end{array} \right] - \frac{2(1-2\eta)\, m}{3\sqrt{3}(1+\eta)} \left(\frac{R_0}{h}\right) \left[\left(\frac{R_a}{R_0}\right) \left\{ 3 - \left(\frac{R_a}{R_0}\right)^2 \right\} - 2 \right] - m \left(\frac{h}{R_0}\right) \quad (19)$$

where $A = \frac{(1-2\eta)^2}{3(1+\eta^2)}$

Results and Discussion

The deformation pattern of metal powder perform is quite different from solid metal deformation. In the powder metal forming operation, there are 2 processes that happen simultaneously, i.e. compaction and deformation. Initially compaction dominates; so the relative average pressure curve increases slowly. After the compaction phase deformation dominates and a steep slope is observed. Material initially flows mainly in the direction of punch movement with little lateral flow. As the density increases, lateral flow increases. In the final stage of deformation the lateral flow approaches the spreading behavior of a pore-free material.

Figure 5 shows that as friction factor increases the relative extrusion pressure increases with increasing extrusion ratio and as L decreases the inner ratios R_i increase tending to equal R_f. Figure 6 shows that relative extrusion pressure also increases with the initial relative density of the preform. The value of $\frac{v_f}{U}$ minimizes the absolute value of the extrusion pressure of Eq. (12). This value also determines the value of R_i, the piping radius, which minimizes the extrusion power. Figures 7 and 8 present the effects of reduction and slug length on the pipe's radius and the relative extrusion pressure. As L decreases, the inner radius R_i increases, tending to equal R_f. An increased value of R_0/R_f requires a higher value of relative extrusion pressure (Figure 7). The experimental result obtained on wrought material (Avitzur, 1979) has been superimposed on the result of metal powder preform (Figure 8).

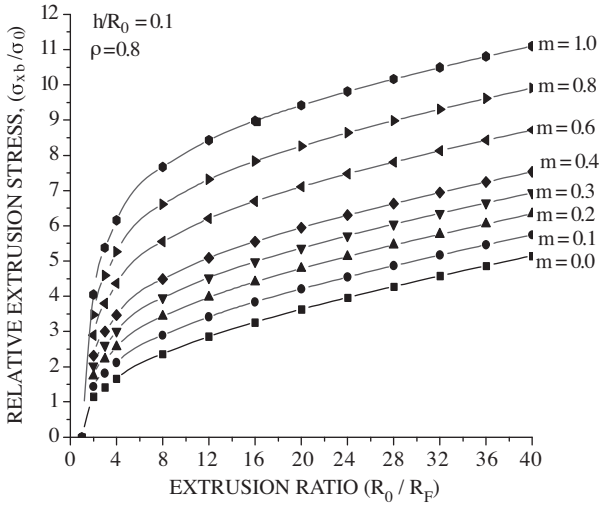

Figure 5. Effect of reduction and constant shear friction force m on extrusion stress at the end of stroke.

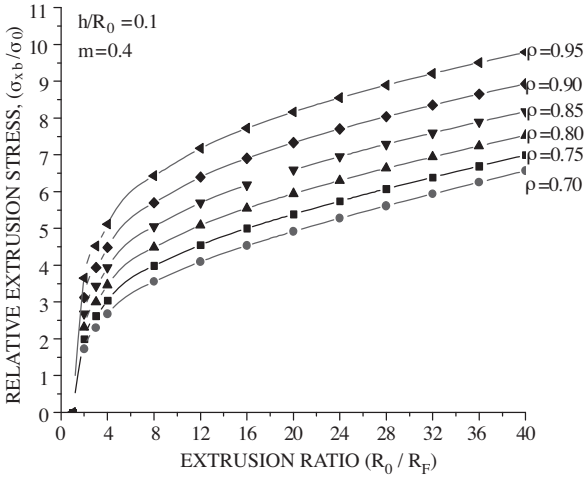

Figure 6. Effect of initial relative density and reduction on extrusion stress at the end of stroke.

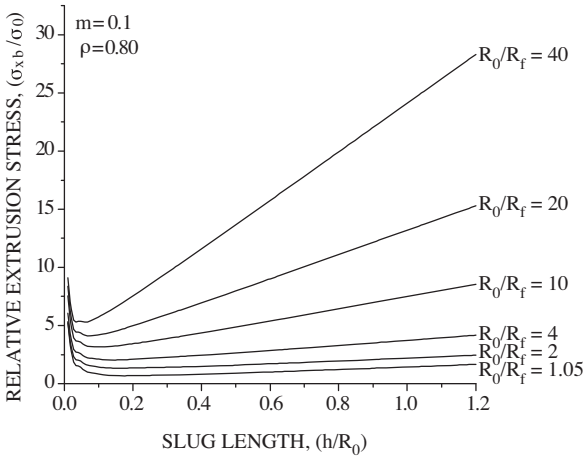

Figure 7. Effect of slug thickness and reduction on relative extrusion stress.

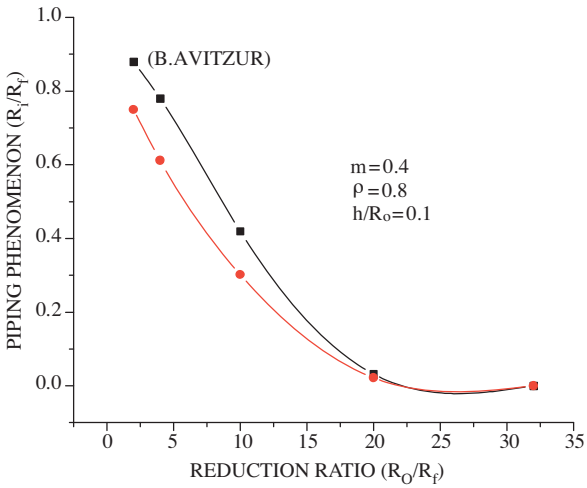

Figure 8. Effect of reduction on the piping phenomenon at the end of stroke.

Figure 8 shows a close agreement of trend during extrusion. Initially there is a large difference between the 2 results. It is due to porosity in the metal powder preform. A large amount of load is consumed initially in densification of the metal powder preform. After attaining $\rho = 1$ asymptotically, the results converge. The density of the preform also increases with the relative extrusion pressure (Figure 9). Initially it increases more, due to dominancy of compaction in the early stage and later it increases less due to plastic deformation. It tends to achieve $\rho = 1$, but it is asymptotic.

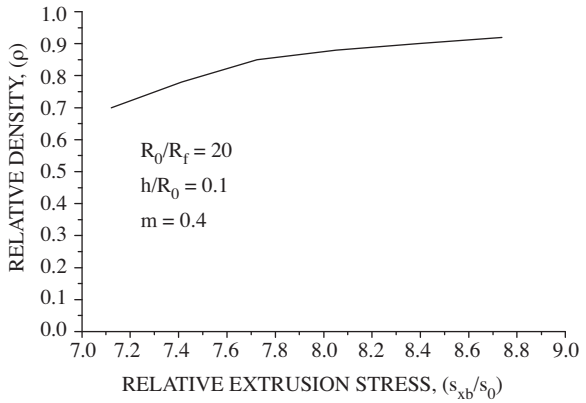

Figure 9. Variation in relative density with relative extrusion stress.

Conclusion

Relative extrusion pressure shows minima at a particular semi-cone angle of the die, and so it can be used as a criterion for forming through conical dies. A lower value of coefficient of friction requires a low value of relative extrusion stress, i.e. it favors the forming operation. A higher initial relative density of the preform needs a lower value of relative extrusion pressure. For a small semi-cone angle, the geometry of the preform does not affect the relative extrusion pressure very much. Therefore, for many reasons, extrusion in practice is performed with cone angles that cause piping defects. Large reductions taken in extrusion require large cone angles as optimal cone angles. To avoid this piping effect at the end of stroke of powder preform the guidelines and/or various process parameters that will affect the forming operation are presented graphically.

Nomenclature

τ	shear stress
μ	coefficient of friction
k	constant equal to 2 in yield criterion
n	a constant quantity much greater than 1
λ	flow stress of metal powder preform
r, θ, z	cylindrical coordinates
ρ	relative density of the preform
ρ_*, ρ_r	densities of apparent and real contact areas
σ_0	yield stress of the non-work hardening matrix metal
$\dot{\varepsilon}_r, \dot{\varepsilon}_\theta, \dot{\varepsilon}_z$	principal strain increment
η	constant and a function of ρ only
R_0	initial radius of the preform
v_0	velocity of preform at zone-1
v_f	final velocity of preform
h	instantaneous length of preform
$\Gamma_1, \Gamma_2, \Gamma_3,$ Γ_4, Γ_5	different boundaries where velocity changes
p	ram pressure
m	friction constant factor

References

Agrawal, M., Kumar, S. and Jha, A.K., "High Speed Forging of Hollow Metal Preforms", J. IE (India)-PR, 80, 8-15, 1999.

Avitzur, B., "Metal Forming Process and Analysis", TMH Publishing Co. Ltd. New Delhi, 269-274, 1979.

Deryagin, B.V., "What is Friction", IZD, AKAD, NAUK, U.S.S.R., 230-234, 1952.

Ilia, E., Tutton, K. and O'Neill, M., "Forging a Way towards a Better Mix of PM Automotive Steels", Metal Powder Report 60, 38-44, 2005.

Jha, A.K. and Kumar, S., "Production of Sintered Forged Components", J. Mater. Process. Tech., 41,143-169, 1994.

Jha, A.K. and Kumar, S., "Rolling of a Metal Powder Preforms Strip", Proc. XI AIMTDR Conf. IIT, Madras, India, 365, 1984.

Kumar, S., Jha, A.K., Singh, R.K. and Singh, S., "Sintered Preforms Adds Better Value to Aerospace Components", J. IE (India) 82, 1-6, 2001.

Ramakrishnan, P., "Forging of Metal Powder Preforms", Proc. Int. Seminar on Metal Working Technology Today an Tomorrow", NIFFT, Ranchi, India, 43-45, 1980.

Rooks, B.W., "The Effect of Die Temperature on Metal Flow and Die Wear during High Speed Hot Forging", 15th Int. MTDR. Conference Held at Birmingham, U.K., 487, Sept. 1974.

Singh, S. and Jha, A., "Sintered Preform Adds Better Value to Aerospace Components", J. Aerospace Eng. I.E. (I),82, 1-6, 2001.

Tabata, T. and Masaki, S., "A Yield Criterion for Porous Metals and Analysis of Axial Compression of Porous Discs", J. Japan Society for Technology of Plasticity, 16, 279, 1975.

Tabata, T., Masaki, S. and K. Hosokawa, "A Compression Test to Determine the Coefficient of Friction in Forging P/M Preforms", Int. J. Powder Metallurgy and Powder Tech., 16, 149, 1980.

Wonklin, T., "Friction at High Normal Pressure", Proc. First WCIT, Paper No. F-7. 1972.